Applied Catalysis B: Environmental 147 (2014) 287–292

Contents lists available at ScienceDirect

Applied Catalysis B: Environmental

journal homepage: www.elsevier.com/locate/apcatb

Inhibition of bromate formation by surface reduction in catalytic ozonation of organic pollutants over β-FeOOH/Al_2O_3

Yulun Nie, Chun Hu*, Nengneng Li, Li Yang, Jiuhui Qu

State Key Laboratory of Environmental Aquatic Chemistry, Research Center for Eco-Environmental Sciences, Chinese Academy of Sciences, Beijing 100085, China

ARTICLE INFO

Article history:
Received 18 July 2013
Received in revised form 2 September 2013
Accepted 3 September 2013
Available online 11 September 2013

Keywords:
BrO_3^- inhibition
β-FeOOH/Al_2O_3
Catalytic ozonation
Surface reduction

ABSTRACT

BrO_3^- formation was investigated over β-FeOOH/Al_2O_3 during the catalytic ozonation of Br^--containing water. The effect of several representative compounds in aqueous environment such as 2,4-dichlorophenoxyacetic acid (2,4-D), phenazone (PZ), diphenhydramine (DP), amitrole (AMT) and Br^--containing raw drinking water was examined on the formation of BrO_3^-. No significant BrO_3^- formation and higher removal of total organic carbon (TOC) were observed during the catalytic ozonation of the tested samples except AMT. Moreover, it was found that the adsorbed BrO_3^- was reduced to Br^-, which was greatly enhanced by the degradation of organics according to the order AMT < DP < PZ < 2,4-D. The surface Fe(II) of β-FeOOH/Al_2O_3 was responsible for the reduction of BrO_3^- on the basis of *in situ* diffuse reflection UV–vis spectra and the determination of surface Fe(II) under different conditions. It was generated from the reaction of surface Fe(III) with $HO_2^{\bullet-}/O_2^{\bullet-}$ during the catalytic ozonation of different pollutants. Furthermore, FTIR and GC–MS analysis verified that the complexation of surface Fe(III) with the oxygen-containing functional groups (—OH, —COOH) of pollutants or their intermediates enhanced the reaction of Fe(III) with $HO_2^{\bullet-}/O_2^{\bullet-}$, resulting in more surface Fe(II) to cause higher BrO_3^- reduction rate. The catalyst still showed effectiveness for the inhibition of BrO_3^- formation and TOC removal for a Br^--containing raw drinking water under the realistic conditions. These findings could be applied to the minimization of BrO_3^- formation in catalytic ozonation of Br^--containing drinking water.

© 2013 Elsevier B.V. All rights reserved.

1. Introduction

The application of ozonation in drinking water treatment is widespread throughout the world, to address water quality problems caused by taste, odor, micropollutants, *etc.* [1]. However, there exists an important scientific challenge: controlling BrO_3^- formation as a result of the ozonation of Br^--containing water [1]. BrO_3^- has been classified as a Group 2B substance (possibly carcinogenic to humans) and the World Health Organization recommends a provisional guideline value of 10 μg/L in drinking water [2].

The mechanism and kinetics of BrO_3^- formation in ozonation have been reported by a number of publications [3]. Br^- is oxidized to HBrO/BrO^- in ozonation, which is further oxidized to BrO_3^- by ozone and/or •OH radicals. Moreover, BrO_3^- formation depends on the ozonation conditions, such as solution pH, ozone contact time, and natural organic matter concentration [3,4]. Three approaches could be used to control BrO_3^- contamination in the water supply: removal of Br^- before BrO_3^- formation *via* membrane filtration and ion exchange [5,6]; control of BrO_3^- formation during ozonation by lowering solution pH or adding H_2O_2 or NH_3 [7,8]; and removal of BrO_3^- after ozonation *via* adsorption or chemical reduction [9–11]. However, a comprehensive technology for the prevention of BrO_3^- contamination has not yet been established in practice for a number of reasons. For example, the rate of •OH radical formation is lowered by pH depression, resulting in a slower degradation rate for organic pollutants [12]. Ammonia addition is unavailable in waters containing medium to high levels of ammonia, because only small ammonia concentrations have a positive effect on the minimization of BrO_3^- formation [4]. The addition of H_2O_2 will impair the disinfection efficiency of ozone due to the enhancement of ozone decomposition. For the technique of using ferrous iron to reduce BrO_3^-, the removal of residual iron from the finished water stream needs to be considered due to the guidelines for iron concentration, which require levels less than 300 μg/L in drinking water [2].

Heterogeneous catalytic ozonation has received increasing attention due to its potentially higher efficiency in the degradation and mineralization of refractory organic pollutants and lower negative effect on water quality compared to other disinfection methods [13]. It was developed to overcome the limitations of ozonation processes, such as formation of byproducts and selective ozone reactions [13,14]. However, only a few studies have been conducted so far concerning the inhibition of BrO_3^- formation in

* Corresponding author. Tel.: +86 10 62849628; fax: +86 10 62923541.
E-mail address: huchun@rcees.ac.cn (C. Hu).

0926-3373/$ – see front matter © 2013 Elsevier B.V. All rights reserved.
http://dx.doi.org/10.1016/j.apcatb.2013.09.005

heterogeneous catalytic ozonation [15,16]. It is necessary to investigate the transformation of bromide in catalytic ozonation in the development of a catalyst for Br^--containing water treatment. Our and other studies have verified that O_3 is decomposed into reactive oxygen species by the interaction of O_3 and the surface hydroxyl groups of catalysts from its surface hydroxylation in aqueous solution [17–19]. Moreover, during the reaction, the catalyst surface was shown to undergo oxidation and reduction, which was similar to the decomposition mechanism of gaseous ozone [20,21]. Therefore, it is worth considering whether surface reduction could be used to prevent BrO_3^- formation during the catalytic ozonation of pollutants.

Akaganeite (β-FeOOH) exhibits a higher BrO_3^- adsorption capacity and selectivity compared with other ions in water [22,23]. In this study, β-FeOOH was supported on mesoporous γ-Al_2O_3 by a hydrothermal hydrolysis process using $FeCl_3{\cdot}6H_2O$ as the metal precursor. Four compounds used as pharmaceuticals or herbicides were selected to evaluate the activity and properties of the catalysts because they exist in the aqueous environment due to their widespread use [24–26], and contain carboxylic acid or carboxylic groups in their initial and byproduct structures. The effect of pollutants on BrO_3^- formation was examined during their catalytic ozonation in β-FeOOH/Al_2O_3 suspension. No significant BrO_3^- formation was observed in β-FeOOH/Al_2O_3 suspension with ozone. Moreover, BrO_3^- was reduced to Br^- at different reaction rates during catalytic ozonation of different organic pollutants. A surface BrO_3^- reduction mechanism was proposed on the basis of *in situ* diffuse reflection UV–vis spectra and analysis of Fe(II) on the catalyst surface under a variety of experimental conditions. These findings will facilitate development of catalytic ozonation for purification of Br^--containing water.

2. Materials and methods

2.1. Materials and reagents

Aluminum *i*-propoxide, glucose and urea were purchased from Beijing Chemical Reagents (Beijing, China). $FeCl_3{\cdot}6H_2O$, $KBrO_3$ and KBr were acquired from Yili Company (Beijing, China). 2,4-Dichlorophenoxyacetic acid (2,4-D), phenazone (PZ), diphenhydramine (DP), and amitrole (AMT) were purchased from Acros (Geel, Belgium) and their molecular structures are also provided (Supplementary Materials Table S1). Oxygen isotope ($^{18}O_2$, >99.8%, CAS: 32767-18-3) was obtained from Beijing Gaisi Chemical Gases Center. All other chemicals were analytical grade and used without further purification. All aqueous solutions were prepared with deionized water.

2.2. Catalyst preparation

β-FeOOH/Al_2O_3 was prepared as described previously [17]. As an example, 0.30 g of $FeCl_3{\cdot}6H_2O$ and 0.40 g urea were dissolved in 3 mL of water, and 2 g Al_2O_3 was added to this solution. The pH was adjusted to 1.6 with hydrochloric acid. Subsequently, the temperature was maintained at 373 K with a water bath for 4 h, and then cooled to room temperature naturally and the sample was washed with deionized water. The catalyst with 3 wt% Fe was used for all subsequent experiments. As a reference, unsupported β-FeOOH was synthesized by the same procedure in the absence of Al_2O_3.

2.3. Characterization

Powder X-ray diffraction (XRD) of the catalyst was recorded on an XDS-2000 Diffractometer (Scintag, Cupertino, CA) with Cu Kα radiation (λ = 1.54059 Å). The X-ray photoelectron spectroscopy (XPS) data of β-FeOOH/Al_2O_3 were taken on an AXIS-Ultra instrument from Kratos using monochromatic Al Kα radiation (225 W, 15 mA, 15 kV) and low-energy electron flooding for charge compensation. To compensate for surface charge effects, the binding energies were calibrated using the C_{1s} hydrocarbon peak at 284.80 eV. *In situ* UV–vis diffuse reflectance (UV–vis DRS) spectra for different catalytic ozonation processes were collected with a Hitachi U-3900 spectrometer with an integrating sphere attachment. The analyzed range was 200–800 nm, and $BaSO_4$ was the reflectance standard. The desired amount of catalyst particles (0.0625 g) was added to 2.5 mL water or ozone solution (2.0 mg/L) and the suspensions were mixed rapidly. The aliquots were immediately withdrawn for UV–vis analysis at different time intervals. $^{18}O_3$ was generated from $^{18}O_2$ in the isotope substitution experiment.

2.4. Procedures and analysis

A 300-mL three-neck flask was used as a reactor and the reaction temperature was maintained at 20 °C. In a typical experiment, 220 mL deionized water was placed into the reactor, which was continuously magnetically stirred, and oxygen-ozone gas was bubbled into the reactor to obtain 2.0 mg/L ozone aqueous solution (the oxygen-ozone gas was stopped when the catalytic ozonation reaction started). Then, the aqueous suspensions with the desired amount of catalyst and organic pollutants, Br^- or BrO_3^- were added into the reactor, which was sealed and magnetically stirred, with a final total volume of 250 mL. In all experiments, the pH of the suspensions was not adjusted during the reaction. In general, the initial suspension pH was about 6, which remained the same within 0.3 units at the end.

Samples were taken at given time intervals (the residual O_3 was liberated by N_2 purging) and filtered through a Millipore filter (pore size 0.45 μm) to remove particles. The filtrates were then divided into several parts for respective measurements of total organic carbon (TOC), BrO_3^- and Br^- by TOC analyzer (TOC-VCPH, SHIMADZU) and ICS-2000 ion chromatography (Dionex Corporations, USA). The ozone was generated by a 3S-A5 laboratory ozonizer (Tonglin Technology, China). All of the experiments were repeated three times.

The surface Fe(II) on β-FeOOH/Al_2O_3 was determined using a phenanthroline spectrophotometric method [27]. 1, 10-Phenanthroline was used as a probe agent for the detection of Fe(II), and could take up Fe(II) from the surface of the solid-phase β-FeOOH/Al_2O_3 *via* a specific chelating reaction. The samples were prepared as follows: the catalyst dispersions under different conditions were filtered and the resulting solid was resuspended in 10 mL of deionized water. After the addition of 1.0 mL of 1, 10-phenanthroline solution and reaction for 10 min, the new dispersion was filtered and the filtrates were analyzed by recording the absorbance at 510 nm. As a reference, no Fe(II) was detected in the filtrates from β-FeOOH/Al_2O_3 dispersions from different reaction conditions. The concentration of ozone dissolved in the aqueous phase was determined with the indigo method [28].

The samples for FTIR were prepared as follows: 0.0625 g β-FeOOH/Al_2O_3 was added into water or different organic pollutant solution (250 mL). The suspension was continuously stirred for 2 h and then filtered. In addition, 0.0625 g β-FeOOH/Al_2O_3 was added into the ozone solution with different organic pollutants, the suspension was continuously stirred for 10 min and then filtered. The above resulting solids were dried at 313 K, and then were mixed with KBr at a fixed ratio (10%). The same amount of mixed powder was also used to prepare the pellets for FTIR. The infrared spectrum was recorded on a TENSOR 27 FTIR spectrophotometer.

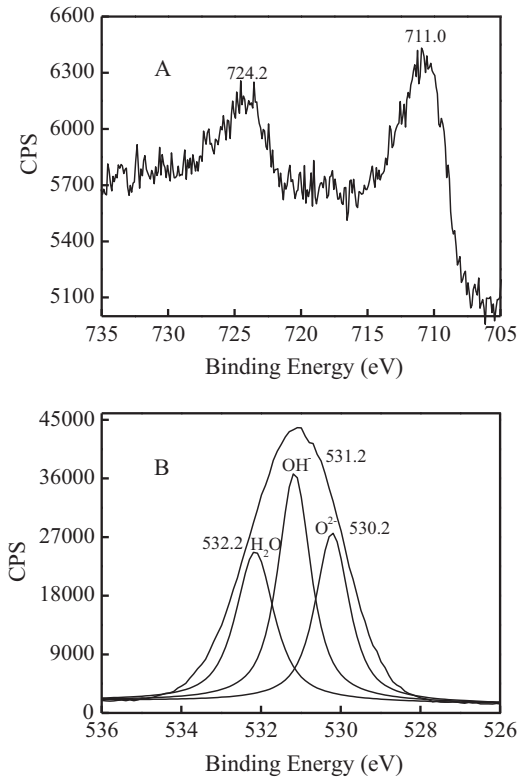

Fig. 1. XPS spectrum of β-FeOOH/Al_2O_3 (A) Fe2p, (B) O1s.

The samples for GC–MS analysis were prepared by the following procedure. The suspensions of β-FeOOH/Al_2O_3 with different pollutants (after reaction 10 min with ozone) were filtered to remove catalyst. The solution was evaporated by the freeze-drying method. The residue was trimethylsilylated with 0.2 mL of anhydrous pyridine, 0.1 mL of hexamethyldisilazane, and 0.05 mL of chlorotrimethylsilane at room temperature. GC–MS analysis was carried out on Agilent 6890GC/5973MSD with a DB-5 MS capillary column.

3. Results and discussion

3.1. Characterization of β-FeOOH/Al_2O_3

Based on the XRD results, no XRD diffraction peaks of β-FeOOH were observed in the supported sample, which was presumably due to its low loading content (3 wt%) and high dispersion on Al_2O_3. However, β-FeOOH was the predominant phase of the unsupported sample prepared by the same method (Supplementary Materials Fig. S1). Therefore, the supported iron oxide should have the same structure as the unsupported one and the supported sample was designated β-FeOOH/Al_2O_3.

The oxidation state of iron species on the surface of β-FeOOH/Al_2O_3 was confirmed by XPS analysis and the results were shown in Fig. 1. The peaks at 711 and 724.2 eV for the binding energies of $Fe2p_{3/2}$ and $Fe2p_{1/2}$ were assigned to Fe(III) species. The O1s region could be decomposed into three peaks at 530.2, 531.2 and 532.2 eV, corresponding to O^{2-}, OH^- and chemically or physically adsorbed water [29]. The existence of surface OH^- groups suggested that Fe(III) was mainly in the state of FeOOH. The above results confirmed that β-FeOOH was supported on the surface of Al_2O_3.

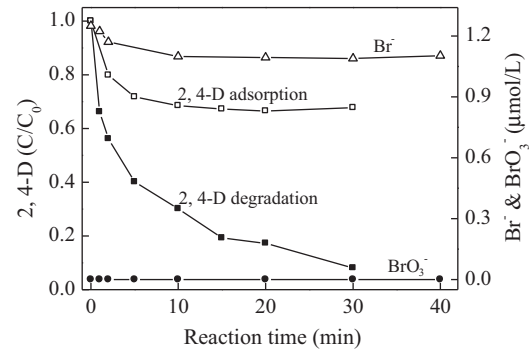

Fig. 2. The changes of BrO_3^- and Br^- concentration during the catalytic ozonation of 2,4-D (10 mg/L) in β-FeOOH/Al_2O_3 suspension. (Initial pH 6.0, catalyst concentration 0.25 g/L, initial concentration of ozone in solution 2.0 mg/L, initial Br^- concentration 1.25 μmol/L.)

3.2. Inhibition of BrO_3^- formation over β-FeOOH/Al_2O_3 with ozone

BrO_3^- formation as a result of Br^- oxidation was examined during the degradation of 2,4-D in ozone alone and β-FeOOH/Al_2O_3 suspension with ozone, respectively. In ozonation alone, the BrO_3^- concentration increased quickly and reached 21.5 μg/L with the oxidation of Br^-, which is considerably above the allowable limit of 10 μg/L, and 2,4-D, TOC removal was decreased to 34% and 7% respectively compared with the values (86% and 26%) in the absence of Br^- (Supplementary Materials Fig. S2). In contrast, as shown in Fig. 2, neither BrO_3^- formation nor Br^- oxidation (The decrease of Br^- concentration could be attributed to the Br^- adsorption on the catalyst) was observed over β-FeOOH/Al_2O_3 with ozone, indicating that the BrO_3^- formation was completely inhibited. Besides, 32% of 2,4-D was adsorbed on β-FeOOH/Al_2O_3, while 92% of 2,4-D was degraded after catalytic ozonation for 30 min, and 64% of TOC was removed, which was slightly higher than that without Br^- (89%, 61%) (Supplementary Materials Fig. S3). Moreover, the BrO_3^- formation was also significantly inhibited over β-FeOOH/Al_2O_3 during the catalytic ozonation of the other pollutants except for AMT, and TOC was removed by 33%, 30% and 13% for PZ, DP and AMT respectively (Supplementary Materials Fig. S4), while their adsorption almost approached zero, and TOC removals were lower in ozone alone. The results indicated that β-FeOOH/Al_2O_3 exhibited both inhibition of BrO_3^- formation and higher efficiency for the elimination of organic pollutants.

Furthermore, with BrO_3^- as the starting compound, the reduction of BrO_3^- was examined over β-FeOOH/Al_2O_3 in catalytic ozonation of 2,4-D. As shown in Fig. 3, about 68% of BrO_3^- was adsorbed on β-FeOOH/Al_2O_3. However, with the addition of ozone, BrO_3^- was completely converted into Br^- during the degradation of 2,4-D within 180 min. On the contrary, neither BrO_3^- reduction nor Br^- formation was observed with the degradation of 2,4-D in ozone alone. The results indicated that the reduction of adsorbed BrO_3^- to Br^- should be responsible for the inhibition of BrO_3^- formation in catalytic ozonation. In addition, the BrO_3^- reduction was determined during the degradation of different organic pollutants in the same system. As shown in Fig. 4, no significant BrO_3^- was reduced without organic pollutants. However, the reduction of BrO_3^- was significantly promoted in the presence of the selected pollutants, except AMT, with the order AMT < DP < PZ < 2,4-D, which was similar to the order of pollutant degradation rates (Supplementary Materials Fig. S5).

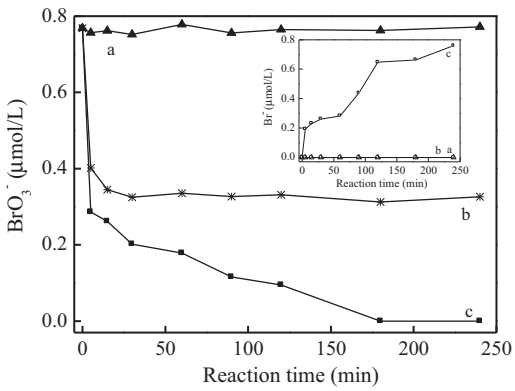

Fig. 3. The changes of BrO_3^- and Br^- concentration (inset) in (a) ozonation, (b) BrO_3^- adsorption and (c) catalytic ozonation on β-FeOOH/Al_2O_3. (Initial pH 6.0, catalyst concentration 0.25 g/L, initial concentration of ozone in solution 2.0 mg/L, initial BrO_3^- concentration 0.78 μmol/L, 2,4-D concentration 10 mg/L.)

3.3. Effective species for BrO_3^- reduction

Tert-butanol, a strong radical scavenger, was adopted as the indicator for the presence of a radical type reaction. The addition of *tert*-butanol markedly reduced the ozonation of 2,4-D in β-FeOOH/Al_2O_3, indicating that the •OH was the main active species in catalytic ozonation (Supplementary Materials Fig. S6).

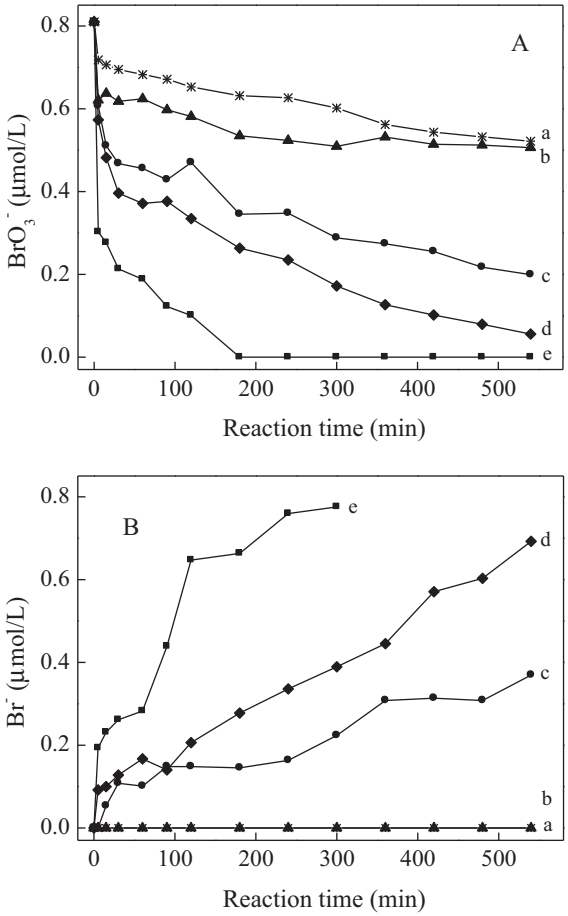

Fig. 4. The changes of BrO_3^- (A) and Br^- and (B) concentration in catalytic ozonation of different pollutants over β-FeOOH/Al_2O_3: (a) without pollutant, (b) AMT, (c) DP, (d) PZ and (e) 2,4-D. (Initial pH 6.0, catalyst concentration 0.25 g/L, initial concentration of ozone in solution 2.0 mg/L, initial BrO_3^- concentration 0.78 μmol/L, pollutants concentration 45.2 μmol/L.)

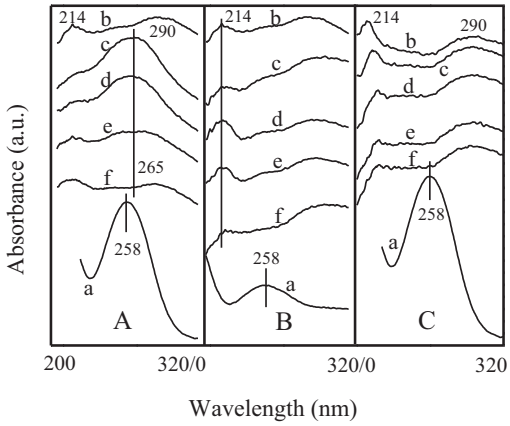

Fig. 5. Time-dependent UV–vis spectra of β-FeOOH/Al_2O_3 suspensions (A) $^{16}O_3$, (B) $^{18}O_3$ and (C) $^{16}O_3 + PO_4^{3-}$. For all panels: (a) O_3, (b) β-FeOOH/Al_2O_3, (c) 1 min, (d) 3 min, (e) 15 min and (f) 40 min for different reaction times.

The results suggested that β-FeOOH/Al_2O_3 accelerated more ozone transformation into •OH radicals. Fig. 5 shows the UV–vis DRS spectra of β-FeOOH/Al_2O_3 suspension with ozone under different conditions. The support Al_2O_3 did not have any absorption in the range 200–320 nm (data not shown), while UV absorbance bands of $^{16}O_3$ and $^{18}O_3$ were observed at 258 nm. In β-FeOOH/Al_2O_3 suspensions, two intense bands appeared at 214 and 290 nm, which were attributed to isolated Fe(III) with tetrahedral (214 nm) and higher coordination numbers (290 nm) [30]. When ozone was added into the β-FeOOH/Al_2O_3 suspensions, both peaks disappeared; meanwhile, a new band centered at 265 nm was observed, which was assigned to low-energy charge transfer between oxygen ligands and the central Fe(III) ion in tetrahedral symmetry [31,32]. Moreover, the peak intensity decreased with reaction time and disappeared at 40 min, and the UV–vis spectra of the catalyst then reverted to the initial one. In addition, when $^{18}O_3$ generated from $^{18}O_2$ was added to the β-FeOOH/Al_2O_3 suspension, only the peak at 214 nm increased and reached a maximum at 3 min, then decreased rapidly and returned to the original intensity at 40 min. However, the UV–vis DRS of β-FeOOH/Al_2O_3 did not change in the presence of phosphate under otherwise identical conditions. It has been verified that O_3 interacts with surface hydrogen-bonded hydroxyl groups and H_2O to initiate reactive oxygen species [17,18]. Since phosphate could substitute for the surface hydroxyl group and chemisorbed water [33], blocking the surface reaction of O_3, the results confirmed that the interaction of O_3 with the surface hydroxyl group and chemisorbed H_2O of the catalyst affected the tetrahedral and higher coordination of Fe(III) and O^{2-} in the framework of β-FeOOH/Al_2O_3. As shown in Fig. 6, no Fe(II) was detected on the surface of β-FeOOH/Al_2O_3 aqueous suspension, while the generation of Fe(II) on the surface of β-FeOOH/Al_2O_3 was observed with the addition of ozone, and the amounts of surface Fe(II) increased greatly in the presence of 2,4-D. Furthermore, the amount of surface Fe(II) decreased rapidly with the addition of BrO_3^-, suggesting that the surface Fe(II) was the effective species in BrO_3^- reduction to Br^- [34,35]. Moreover, Fig. 7 showed that the surface Fe(II) formation reached a maximum of 3.39 μmol/g with catalytic ozonation of 2,4-D at 15 min, and then decreased gradually to 0.35 μmol/g at 240 min, indicating that the amount of surface Fe(II) available for the reduction of BrO_3^- was relatively stable. In addition, about 50% of BrO_3^- was reduced with catalytic ozonation of 2,4-D at initial pH 4 and 7.5, while about 96% of BrO_3^- was reduced at initial pH 6.5 (Supplementary Materials Fig. S7). The effect of initial pH can be predominantly attributed to the formation and transformation of the surface Fe(II) during the degradation of 2,4-D. In the presence of different organic compounds,

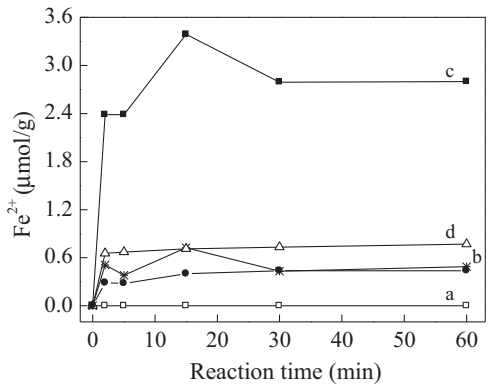

Fig. 6. Determination of surface Fe(II) on β-FeOOH/Al_2O_3 under different conditions: (a) without O_3, (b) with O_3, (c) with O_3 and 2,4-D and (d) with O_3, 2,4-D and BrO_3^-. (Initial pH 6.0, catalyst concentration 0.25 g/L, initial concentration of ozone in solution 2.0 mg/L, initial BrO_3^- concentration 0.78 μmol/L, 2,4-D concentration 10 mg/L.)

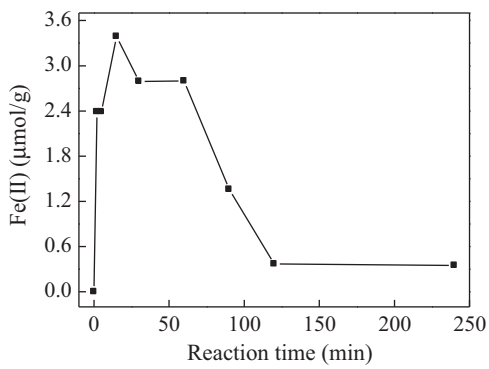

Fig. 7. Determination of surface Fe(II) on β-FeOOH/Al_2O_3 in the presence of O_3 and 2,4-D. (Initial pH 6.0, catalyst concentration 0.25 g/L. (Initial concentration of ozone in solution 2.0 mg/L, 2,4-D concentration 10 mg/L.)

the amounts of surface Fe(II) increased according to the order: AMT < DP < PZ < 2,4-D (Fig. 8), which agreed well with the results of BrO_3^- reduction. The results indicated that the surface Fe(III) of the catalyst was reduced to Fe(II) during the decomposition of ozone in β-FeOOH/Al_2O_3 suspension, and the degradation of pollutants increased the reduction of Fe(III). Furthermore, the role of different organic pollutants and their byproducts in the surface Fe(II) formation during catalytic ozonation was investigated. Fig. 9 showed the FTIR spectra of 2,4-D and β-FeOOH/Al_2O_3-adsorbed 2,4-D.

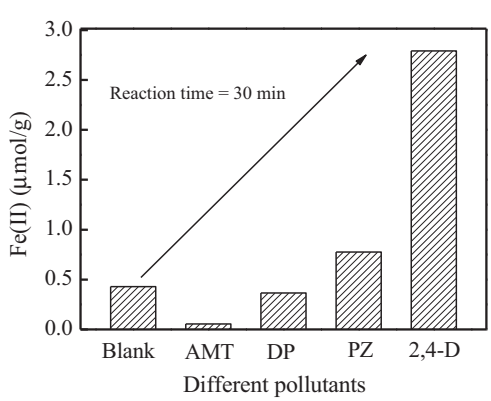

Fig. 8. Determination of surface Fe(II) on β-FeOOH/Al_2O_3 during the catalytic ozonation of different pollutants. (Initial pH 6.0, catalyst concentration 0.25 g/L. (Initial concentration of ozone in solution 2.0 mg/L, initial pollutants concentration 45.2 μmol/L.)

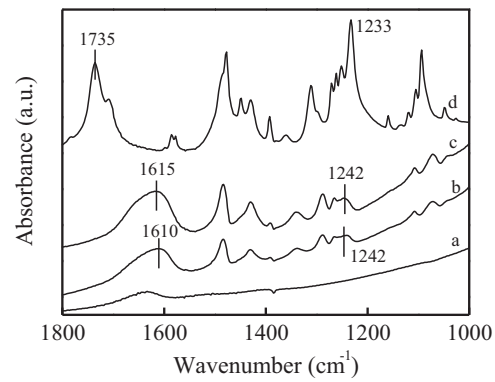

Fig. 9. FTIR spectra of β-FeOOH/Al_2O_3 before and after adsorbing 2,4-D: (a) catalyst, (b) 2,4-D-adsorbed Al_2O_3, (c) 2,4-D-adsorbed catalyst and (d) 2,4-D.

The characteristic peaks of carboxylic acid groups (1735 cm^{-1}) and C-O of carboxylic functional groups (1233 cm^{-1}) appeared for 2,4-D [36]. Moreover, the above peaks shifted markedly to 1615 and 1242 cm^{-1} for 2,4-D adsorbed on β-FeOOH/Al_2O_3, while they became 1610 and 1242 cm^{-1} for 2,4-D adsorbed on Al_2O_3. Moreover, the former peak intensity was higher than the latter one, indicating the presence of complex formation between the O atom in carboxylic groups and Fe atoms in β-FeOOH/Al_2O_3 [37]. By contrast, no functional group complexation with Fe appeared for AMT and its byproducts, so no complex was formed when AMT was added to the β-FeOOH/Al_2O_3 suspension (Supplementary Materials Fig. S8). However, the complexation of oxygen functional groups (—OH, —COOH) with metal was observed by GC–MS analysis for 2,4-D, PZ, DP and their byproducts in catalytic ozonation (Supplementary Materials Table S2). Therefore, the complexation of Fe(III) in β-FeOOH/Al_2O_3 with organic ligands occurred during the catalytic ozonation of 2,4-D, PZ and DP, which has been verified by the 1637 cm^{-1} peak of carboxylic groups appearing in FTIR spectra of used β-FeOOH/Al_2O_3 for these pollutants (Supplementary Materials Fig. S9). Clearly, the surface Fe(II) formation was enhanced by the complexation of organic groups with Fe(III) of β-FeOOH/Al_2O_3. During the interaction of O_3 and β-FeOOH/Al_2O_3, adsorbed $HO_2^{\bullet-}/O_2^{\bullet-}$ could be generated according to the previous work [17,20,38,39]. The surface Fe(III) was reduced to Fe(II) by reaction with $HO_2^{\bullet-}/O_2^{\bullet-}$, with a rate constant of 1.4×10^5 M^{-1} s^{-1} [40]. It has been reported that the complexation of Fe(III) with ligands can decrease the Fe(III)/Fe(II) redox potential (*e.g.*, from 0.77 to 0.628, 0.256 V (*vs* NHE) for acetate, oxalate) [41]. The complexation of surface Fe(III) with pollutants or their intermediates (containing —OH, —COOH) enhanced the reaction rate constant of Fe(III) with $HO_2^{\bullet-}/O_2^{\bullet-}$ (2.0×10^6 M^{-1} s^{-1} in the presence of ligands) [42], resulting in more surface Fe(II) generation during the catalytic ozonation of pollutants. The surface Fe(II) was responsible for the reduction of adsorbed BrO_3^- to Br^-, thus resulting in inhibition of BrO_3^- formation in the catalytic ozonation process.

In order to evaluate the catalyst performance under the realistic conditions, a Br^--containing raw drinking water was used to investigate BrO_3^- formation and TOC removal in catalytic ozonation and ozonation process. In the raw water (Supplementary Materials Table S3), the concentration of TOC and Br^- was 3.6 mg/L and 1.07 μmol/L, and the alkalinity was 190 mg/L ($CaCO_3$). In β-FeOOH/Al_2O_3 suspension with an initial concentration of 2.0 mg/L ozone, neither BrO_3^- formation nor significant Br^- oxidation was observed, while 30% of TOC were removed (Fig. 10). For the same water, 0.539 μmol/L BrO_3^- was formed, and only 7% of TOC was removed in ozonation alone (Supplementary Materials Fig. S10), while 0.273 μmol/L BrO_3^- was formed in Al_2O_3 suspension (Supplementary Materials Fig. S11). Besides, the addition of 2,4-D in the

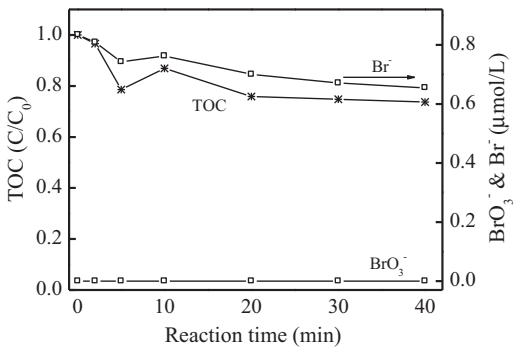

Fig. 10. The changes of BrO_3^- and Br^- concentration in catalytic ozonation of Br^--containing raw drinking water over β-FeOOH/Al_2O_3. (Initial pH 8.0, catalyst concentration 0.25 g/L, initial concentration of ozone in solution 2.0 mg/L.)

raw water was further used as a probe compound to compare the oxidation capacity in the above two systems. 95% and 76% of 2,4-D were removed over β-FeOOH/Al_2O_3 with ozone and in ozonation alone, respectively. The results above indicated that the effect of carbonate in water on the ozonation efficiency was slight (Supplementary Materials Fig. S12). Thus, β-FeOOH/Al_2O_3 is a promising ozonation catalyst for the purification of Br^--containing water.

4. Conclusions

β-FeOOH/Al_2O_3 exhibited both significant inhibition of BrO_3^- formation and higher efficiency toward the catalytic ozonation of organic pollutants in water. Besides, the adsorbed BrO_3^- could be reduced to Br^- and it was greatly enhanced by the degradation of organics according to the order AMT < DP < PZ < 2,4-D. It was confirmed that the surface Fe(II) of β-FeOOH/Al_2O_3 generated from the reaction of surface Fe(III) with $HO_2^{\bullet-}/O_2^{\bullet-}$ was responsible for the reduction of BrO_3^-. Moreover, the complexation of surface Fe(III) with the oxygen functional groups (—OH, —COOH) of pollutants or their intermediates enhanced the reaction of Fe(III) with $HO_2^{\bullet-}/O_2^{\bullet-}$, resulting in more surface Fe(II) to cause higher BrO_3^- reduction rate. β-FeOOH/Al_2O_3 still showed effectiveness for the inhibition of BrO_3^- formation and TOC removal for a Br^--containing raw drinking water sample under the realistic conditions.

Acknowledgements

This work was supported by the 973 project (No. 2010CB933604) and the National Natural Science Foundation of China (No. 21125731, 51138009, 51278527).

Appendix A. Supplementary data

Supplementary data associated with this article can be found, in the online version, at http://dx.doi.org/10.1016/j.apcatb.2013.09.005.

References

[1] R.P. Schwarzenbach, B.I. Escher, K. Fenner, T.B. Hofstetter, C.A. Johnson, U. Gunten, B. Wehrli, Science 313 (2006) 1072–1077.
[2] WHO, Guidelines for Drinking-Water Quality: Incorporating First Addendum, WHO Press, Geneva, 2006.
[3] U. von Gunten, J. Hoigne, Environmental Science and Technology 28 (1994) 1234–1242.
[4] U. Pinkernell, U. von Gunten, Environmental Science and Technology 35 (2001) 2525–2531.
[5] S. Chellam, Environmental Science and Technology 34 (2000) 1813–1820.
[6] N.I. Chubar, V.F. Samanidou, V.S. Kouts, G.G. Gallios, V.A. Kanibolotsky, V.V. Strelko, I.Z. Zhuravlev, Journal of Colloid and Interface Science 291 (2005) 67–74.
[7] U. von Gunten, Y. Oliveras, Environmental Science and Technology 32 (1998) 63–70.
[8] R. Hofmann, R.C. Andrews, Water Research 40 (2006) 3343–3348.
[9] W. Chen, Z. Zhang, Q. Li, H. Wang, Chemical Engineering Journal 203 (2012) 319–325.
[10] N. Kishimoto, N. Nobuaki, Environmental Science and Technology 43 (2009) 2054–2059.
[11] R. Butler, A. Godley, L. Lytton, E. Cartmell, Critical Reviews in Environment Science and Technology 35 (2005) 193–217.
[12] M. Deborde, S. Rabouan, J.P. Duguet, B. Legube, Environmental Science and Technology 39 (2005) 6086–6092.
[13] J. Nawrocki, B. Kasprzyk-Hordern, Applied Catalysis B: Environmental 99 (2010) 27–42.
[14] J. Benner, T.A. Ternes, Environmental Science and Technology 43 (2009) 5086–5093.
[15] T. Zhang, W. Chen, J. Ma, Z. Qiang, Water Research 42 (2008) 3651–3658.
[16] T. Zhang, P. Hou, Z. Qiang, X. Lu, Q. Wang, Chemosphere 82 (2011) 608–612.
[17] L. Yang, C. Hu, Y. Nie, J. Qu, Applied Catalysis B: Environmental 97 (2010) 340–346.
[18] L. Zhao, Z. Sun, J. Ma, H. Liu, Environmental Science and Technology 43 (2009) 4157–4163.
[19] M. Ernst, F. Lurot, J.C. Schrotter, Applied Catalysis B: Environmental 47 (2004) 15–25.
[20] W. Li, G.V. Gibbs, S.T. Oyama, Journal of the American Chemical Society 120 (1998) 9041–9046.
[21] A. Lv, C. Hu, Y. Nie, J. Qu, Applied Catalysis B: Environmental 117/118 (2012) 246–252.
[22] R. Chitrakar, S. Tezuka, A. Sonoda, K. Sakane, T. Hirotsu, Industrial and Engineering Chemistry Research 48 (2009) 2107–2112.
[23] C. Xu, J. Shi, W. Zhou, B. Gao, Q. Yue, X. Wang, Chemical Engineering Journal 187 (2012) 63–68.
[24] E. Brillas, J.C. Calpe, P.L. Cabot, Applied Catalysis B: Environmental 46 (2003) 381–391.
[25] T. Heberer, Journal of Hydrology 266 (2002) 175–189.
[26] M.A. Fontecha-Cámara, M.A. Álvarez-Merino, F. Carrasco-Marín, M.V. López-Ramón, C. Moreno-Castilla, Applied Catalysis B: Environmental 101 (2011) 425–430.
[27] J. Wu, H. Zhang, J. Qiu, Journal of Hazardous Materials 215/216 (2012) 138–145.
[28] H. Bader, J. Hoigne, Water Research 15 (1980) 449–456.
[29] D.T. Harvey, R.W. Linton, Analytical Chemistry 53 (1981) 1684–1688.
[30] M.S. Kumar, M. Schwidder, W. Grunert, A. Bruckner, Journal of Catalysis 227 (2004) 384–397.
[31] Y. Wang, Q. Zhang, T. Shishido, K. Takehira, Journal of Catalysis 209 (2002) 186–196.
[32] A. Vinu, T. Krithiga, V. Murugesan, M. Hartmann, Advanced Materials 16 (2004) 1817–1821.
[33] M.I. Tejedor-Tejedor, M.A. Anderson, Langmuir 2 (1986) 203–210.
[34] L. Xie, C. Shang, Q. Zhou, Journal of Environmental Sciences 20 (2008) 257–261.
[35] R. Chitrakar, Y. Makita, A. Sonoda, T. Hirotsu, Journal of Colloid and Interface Science 354 (2011) 798–803.
[36] E.I. Seck, J.M. Dona-Rodriguez, C. Fernandez-Rodríguez, O.M. Gonzalez-Diaz, J. Arana, J. Perez-Pena, Applied Catalysis B: Environmental 125 (2012) 28–34.
[37] N. Wang, L. Zhu, M. Lei, Y. She, M. Cao, H. Tang, ACS Catalysis 1 (2011) 1193–1202.
[38] J. Staehelln, J. Hoigne, Environmental Science and Technology 16 (1982) 676–681.
[39] R.E. Buhler, J. Staehelln, J. Hoigne, Journal of Physical Chemistry B 88 (1984) 2560–2564.
[40] X. Xue, K. Hannaa, C. Despasa, F. Wu, N. Deng, Journal of Molecular Catalysis A: Chemical 311 (2009) 29–35.
[41] T.J. Strathmann, A.T. Stone, Environmental Science and Technology 36 (2002) 5172–5183.
[42] B.G. Kwon, E.J. Kim, J.H. Lee, Chemosphere 74 (2009) 1335–1339.